1 Supplementary tables

The new calibration of climate reconstruction for Mongolia and Siberia presented in this study is based up on the New Mongolia-Siberia Data Base (NMSDB). Published br–GDGT/climate calibration equations are tested on the (NMSDB) (S1). Location, ecosystems as well as sample type are provided in Table (S2). All the br–GDGTs mr–models discussed in this study are presented in the table (S3).

Table S1. Synthesis of the formulae for the main indexes br–GDGT fractional abundances.

Indice	Formula	Proxy purpose	Reference
MBT	$= \dfrac{Ia+Ib+Ic}{\sum brgdgt}$	Temperature, Precipitation, pH	Weijers et al. (2007), Huguet et al. (2013)
MBT′	$= \dfrac{Ia+Ib+Ic}{Ia+Ib+Ic+IIa'+IIa''+IIb+IIb'+IIc'+IIc''+IIIa'+IIIa''+IIIb'+IIIb''+IIIc'}$	Temperature, Precipitation	Peterse et al. (2012)
MBT′$_{5Me}$	$= \dfrac{Ia+Ib+Ic}{Ia+Ib+Ic+IIa+IIb+IIc+IIIa}$	Temperature, Precipitation	De Jonge et al. (2014b)
CBT	$= -\log\left(\dfrac{Ib+IIb+IIb'}{Ia+IIa+IIa'}\right)$	pH	Weijers et al. (2007)
CBT$_{5Me}$	$= -\log\left(\dfrac{Ib+IIb}{Ia+IIa}\right)$	pH	De Jonge et al. (2014b)
CBT′	$= -\log\left(\dfrac{Ic+IIa'+IIb'+IIc'+IIIa'+IIIb'+IIIc'}{Ia+IIa+IIIa}\right)$	pH	De Jonge et al. (2014b)
R$_{i/b}$	$= \dfrac{IV+IV'+V+VI+VII+VIII}{Ia+Ib+Ic+IIa+IIb+IIc+IIIa+IIIb+IIIa}$	Aridity	Xie et al. (2012), Yang et al. (2014)
BIT	$= \dfrac{Ia+IIa+IIIa+IIa'+IIIa'+IIa''+IIIa''+IIIa'''}{Ia+IIa+IIIa+IIa'+IIIa'+IIa''+IIIa''+Cren}$	Lake / Basin OM^{b} production	Hopmans et al. (2004)
II/III	$= \dfrac{IIa}{IIIa}$	Lake / Basin OM production	Xiao et al. (2016)
$MAAT_{MBTp-DJ}$	$= 0.81 - 5.67 \times CBT + 31 \times MBT'$	Soils	Peterse et al. (2012)
$MAAT_{DJ-5Me}$	$= -8.57 + 31.45 \times MBT'_{5Me}$	Soils	De Jonge et al. (2014a)
$MAAT_{soil-Naaf}$	$= 40.01 \times MBT'_{5Me} - 15.25$	Soils	Naafs et al. (2017)
$MAAT_{soil5Me-Naaf}$	$= 39.09 \times MBT'_{5Me} - 14.5$	Soils	Naafs et al. (2017)
$MAAT_{bog5Me-Naaf}$	$= 52.18 \times MBT'_{5Me} - 23.05$	Peat	Naafs (2017)
$MAAT_{Ding}$	$= -2.68 + 26.14 \times MBT - 3.37 \times CBT$	Soils	Ding et al. (2015)
$MAAT_{Wang}$	$= 27.63 \times Index1 - 5.72$	Soils	Wang et al. (2016)
$MAAT_{mr-DJ}$	$= 7.17 + 17.1 \times [Ia] + 25.9 \times [Ib] + 34.4 \times [Ic] - 28.6 \times [IIa]$	Soils	De Jonge et al. (2014a)
$MAAT_{mr-Yang}$	$= 20.9 - 13.4 \times [IIa] - 17.2 \times [IIIa] - 17.5 \times [IIb] + 11.2 \times [Ib]$	Soils	Yang et al. (2014)
$MAAT_{mr-Tibet}$	$= 20.87 - 18.04 \times [IIIa] + 38.88 \times [IIb] - 12.92 \times [IIa] - 20.41 \times [IIb] - 30.27 \times [IIc] + 12.94 \times [Ib]$	Soils	Thomas et al. (2017)
$MAAT_{L.Sun}$	$= 3.949 - 5.593 \times CBT + 38.213 \times MBT$	Lake	Sun et al. (2011)

Table S2. Sample sites included in the New Mongolia-Siberia DataBase (NMSDB).

Site Label	Lat.	Long.	Elev.	Pollen	GDGT	Type used in Fig.	Biomes
MMNT1M01	48.3983	106.8594	1137	Moss polster	Soil part of moss litter	Moss	Steppe-forest
MMNT1M02	48.4014	106.8613	1161	Moss polster	Soil part of moss litter	Moss	Steppe-forest
MMNT2M01	48.4472	107.0542	1438	Moss polster	Soil part of moss litter	Moss	Steppe-forest
MMNT2M02	48.4460	107.0551	1333	Moss polster	Soil part of moss litter	Moss	Steppe-forest
MMNT2M03	48.4449	107.0564	1265	Moss polster	Soil part of moss litter	Moss	Steppe-forest
MMNT2M04	48.4441	107.0580	1266	Moss polster	Soil part of moss litter	Moss	Light taiga
MMNT2M05	48.4425	107.0593	1262	Moss polster	**Unused**	Moss	Light taiga
MMNT2M05'	48.4444	107.0634	1273	Moss polster	Soil part of moss litter	Moss	Light taiga
MMNT2M06	48.4412	107.0629	1328	Moss polster	Soil part of moss litter	Moss	Light taiga
MMNT2M07	48.4381	107.0660	1475	Moss polster	Soil part of moss litter	Moss	Steppe-forest
MMNT3S01	47.2993	103.6092	1323	Soil	Soil	Soil	Steppe
MMNT3S02	47.2000	102.8438	1457	Soil	Soil	Soil	Steppe
MMNT3M03	46.8239	102.2307	1669	Moss polster	Soil part of moss litter	Moss	Alpine meadow
MMNT3M04	46.7932	102.0868	1734	Moss polster	Soil part of moss litter	Moss	Alpine meadow
MMNT3S05	46.7800	101.9510	1830	Soil	Soil	Soil	Alpine meadow
MMNT4S01	45.6645	101.6054	1750	Soil	Soil	Soil	Steppe-desert
MMNT4S02	45.1759	101.4288	1238	Soil	Soil	Soil	Desert
MMNT4S03	45.1724	101.4517	1233	Soil	Soil	Soil	Desert
MMNT4S04	45.1702	101.4806	1230	Soil	Soil	Soil	Desert
MMNT4S05	45.1618	101.4927	1228	Soil	Soil	Soil	Desert
MMNT4S06	45.1467	101.5083	1230	Soil	Soil	Soil	Desert
MMNT4S07	45.1402	101.5087	1232	Soil	Soil	Soil	Desert
MMNT4S08	44.6746	102.1844	1508	Soil	Soil	Soil	Steppe-desert
MMNT4M09	44.4509	102.3459	1847	Moss polster	Soil part of moss litter	Moss	Steppe-desert
MMNT4M10	44.3952	102.4511	1677	Moss polster	Soil part of moss litter	Moss	Steppe-desert
MMNT4S11	44.1685	102.6031	1273	Soil	Soil	Soil	Desert
MMNT4S12	43.9494	102.7411	1574	Soil	Soil	Soil	Steppe-desert
MMNT4S13	43.8636	102.7479	1802	**Unused**	Soil	Soil	Steppe-desert
MMNT4S14	43.7650	102.8018	1982	Soil	Soil	Soil	Steppe-desert
MMNT5C01	48.4074	101.8797	1433	Pond mud	Pond mud	Mud	Alpine meadow
MMNT5C03	48.6592	101.2015	1579	Pond mud	Pond mud	Mud	Alpine meadow
MMNT5M04	48.4136	102.2389	1566	Moss polster	Soil part of moss litter	Moss	Steppe
MMNT5M05	48.4203	102.2266	1538	Moss polster	Soil part of moss litter	Moss	Steppe
MMNT5M06	47.7340	101.2459	1646	Moss polster	**Unused**	Moss	Steppe-forest
MMNT5M07	47.7338	101.2460	1647	Moss polster	**Unused**	Moss	Steppe-forest
MMNT5C11	48.9290	101.9588	1316	Lake Top-core	**Unused**	Lake sediment	Steppe-forest
MMNT5C12	48.6907	101.4263	1436	**Lake Top-core**	**Cross-value**	**Lake sediment**	Steppe-forest
MRUT1M01	52.0497	104.1132	565	Moss polster	Soil part of moss litter	Moss	Dark taiga
MRUT1M02	52.0498	104.1137	574	Moss polster	Soil part of moss litter	Moss	Dark taiga
MRUT1M03	52.0493	104.1132	582	Moss polster	Soil part of moss litter	Moss	Light taiga
MRUT1M04	52.0500	104.1140	557	Moss polster	Soil part of moss litter	Moss	Dark taiga
MRUT1M05	52.0328	104.2263	640	Moss polster	Soil part of moss litter	Moss	Light taiga
MRUT1M06	52.0148	104.2612	554	Moss polster	Soil part of moss litter	Moss	Dark taiga
MRUT1M07	52.0046	104.3738	476	Moss polster	Soil part of moss litter	Moss	Dark taiga
MRUT1M08	51.9952	104.4023	471	Moss polster	Soil part of moss litter	Moss	Light taiga
MRUT1M09	51.9900	104.4025	473	Moss polster	Soil part of moss litter	Moss	Dark taiga
MRUT1M10	51.9392	104.4636	538	Moss polster	Soil part of moss litter	Moss	Light taiga
MRUT1M11	51.9119	104.5331	725	Moss polster	Soil part of moss litter	Moss	Light taiga
MRUT1M12	51.8797	104.6266	772	Moss polster	Soil part of moss litter	Moss	Light taiga
Total				**48**	**44**	**49**	

3

Table S3. Statistical values and equations of all the br–GDGT MAAT_{mr} and MAP_{mr} models.

Model	k	R^2	RMSE	AIC	Formula
MAAT_{mr1}	1	0.38	1.5	168.4	$\text{MAAT}_{\text{mr1}} = -0.5 \times 1 + 12.9 \times [\text{IIIa}']$
MAAT_{mr2}	2	0.52	1.4	162.6	$\text{MAAT}_{\text{mr2}} = -0.7 \times 1 + 13.4 \times [\text{IIIa}'] + 11.8 \times [\text{IIIb}]$
$\text{MAAT}_{\text{mr3}}{}^{a}$	3	0.57	1.3	156.4	$\text{MAAT}_{\text{mr3}} = 0.6 \times 1 - 25.1 \times [\text{IIIa}] + 12.3 \times [\text{IIIa}'] + 7.2 \times [\text{Ib}]$
MAAT_{mr4}	5	0.62	1.2	**152.6**	$\text{MAAT}_{\text{mr4}} = 4.5 \times 1 - 36.8 \times [\text{IIIa}] + 7.3 \times [\text{IIIa}'] - 37.2 \times [\text{IIIc}] - 24 \times [\text{IIb}] - 5.2 \times [\text{Ia}]$
$\text{MAAT}_{\text{mr5}}{}^{b}$	7	0.66	**1.1**	153.9	$\text{MAAT}_{\text{mr5}} = 4.8 \times 1 - 38.5 \times [\text{IIIa}] + 7.9 \times [\text{IIIa}'] - 27.3 \times [\text{IIIc}] - 3.3 \times [\text{IIa}'] - 26.3 \times [\text{IIb}] + 8.5 \times [\text{IIb}'] - 5.6 \times [\text{Ia}]$
MAAT_{mr6}	9	0.67	**1.1**	155.7	$\text{MAAT}_{\text{mr6}} = 12.3 \times 1 - 52.1 \times [\text{IIIa}] - 16.9 \times [\text{IIIb}] - 25.9 \times [\text{IIIb}'] - 41.1 \times [\text{IIIc}] - 6 \times [\text{IIa}] - 10.4 \times [\text{IIa}'] - 38.5 \times [\text{IIb}] - 13.3 \times [\text{Ia}] - 32.8 \times [\text{Ic}]$
MAAT_{mr7}	10	0.68	**1.1**	157.2	$\text{MAAT}_{\text{mr7}} = 12.3 \times 1 - 52.6 \times [\text{IIIa}] - 16.8 \times [\text{IIIb}] - 25.3 \times [\text{IIIb}'] - 35.7 \times [\text{IIIc}] - 6 \times [\text{IIa}] - 10.5 \times [\text{IIa}'] - 37.8 \times [\text{IIb}] - 15.4 \times [\text{IIc}] - 13.2 \times [\text{Ia}] - 31.4 \times [\text{Ic}]$
MAAT_{mr8}	12	**0.69**	**1.1**	160.5	$\text{MAAT}_{\text{mr8}} = 12.5 \times 1 - 54.9 \times [\text{IIIa}] - 23.6 \times [\text{IIIb}] - 26.8 \times [\text{IIIb}'] - 35.1 \times [\text{IIIc}] - 23.4 \times [\text{IIIc}'] - 5.9 \times [\text{IIa}] - 10.4 \times [\text{IIa}'] - 40.6 \times [\text{IIb}] - 16 \times [\text{IIc}] - 13.5 \times [\text{Ia}] + 5.6 \times [\text{Ib}] - 35.8 \times [\text{Ic}]$
MAAT_{mr9}	15	**0.69**	**1.1**	166.2	$\text{MAAT}_{\text{mr9}} = 10.4 \times 1 - 49.5 \times [\text{IIIa}] + 3.3 \times [\text{IIIa}'] - 21.5 \times [\text{IIIb}] - 26.2 \times [\text{IIIb}'] - 30.9 \times [\text{IIIc}] - 23.3 \times [\text{IIIc}'] - 4.4 \times [\text{IIa}] - 8.9 \times [\text{IIa}'] - 38.1 \times [\text{IIb}] + 0.3 \times [\text{IIb}'] - 13.2 \times [\text{IIc}] + 0 \times [\text{IIc}'] - 11.1 \times [\text{Ia}] + 7.7 \times [\text{Ib}] - 31.7 \times [\text{Ic}]$
MAP_{mr1}	1	0.34	112	546.1	$\text{MAP}_{\text{mr1}} = 179.3 \times 1 + 509.1 \times [\text{Ia}]$
MAP_{mr2}	2	0.51	96.1	534.6	$\text{MAP}_{\text{mr2}} = 59.6 \times 1 + 2289.9 \times [\text{IIb}'] + 710.8 \times [\text{Ia}]$
MAP_{mr3}	3	0.58	91.3	532.1	$\text{MAP}_{\text{mr3}} = 94.1 \times 1 + 2319.7 \times [\text{IIb}'] + 702.2 \times [\text{Ia}] - 3752.5 \times [\text{Ic}]$
MAP_{mr4}	5	0.65	82	526.7	$\text{MAP}_{\text{mr4}} = 245.1 \times 1 - 666.7 \times [\text{IIIa}'] + 2431.9 \times [\text{IIb}'] + 396.2 \times [\text{Ia}] - 276 \times [\text{Ib}] - 3780 \times [\text{Ic}]$
MAP_{mr5}	8	0.69	75.9	525.8	$\text{MAP}_{\text{mr5}} = -103.8 \times 1 + 1553.4 \times [\text{IIIa}] + 536 \times [\text{IIIb}] - 3145.6 \times [\text{IIIb}'] + 2480.3 \times [\text{IIIc}] + 1290.1 \times [\text{IIb}] + 2459.3 \times [\text{IIb}'] + 927.9 \times [\text{Ia}] - 2955.3 \times [\text{Ic}]$
$\text{MAP}_{\text{mr6}}{}^{a}$	10	0.73	72.5	525.8	$\text{MAP}_{\text{mr6}} = -511.3 \times 1 + 1205.9 \times [\text{IIIa}] + 1387.2 \times [\text{IIIb}] + 738.8 \times [\text{IIa}] + 969.8 \times [\text{IIa}'] + 1957.1 \times [\text{IIb}] + 3006.3 \times [\text{IIb}'] + 2406.4 \times [\text{IIc}] + 2003.1 \times [\text{IIc}'] + 1081.7 \times [\text{Ia}] - 2406.3 \times [\text{Ic}]$
$\text{MAP}_{\text{mr7}}{}^{b}$	12	0.75	68.5	**524.8**	$\text{MAP}_{\text{mr7}} = -502.6 \times 1 + 1359.5 \times [\text{IIIa}] + 2462.5 \times [\text{IIIb}] - 2178.3 \times [\text{IIIb}'] + 657.7 \times [\text{IIa}] + 986.8 \times [\text{IIa}'] + 2440.5 \times [\text{IIb}] + 3423.5 \times [\text{IIb}'] + 2831.2 \times [\text{IIc}] + 1967.2 \times [\text{IIc}'] + 1150.2 \times [\text{Ia}] - 955.6 \times [\text{Ib}] - 2103.4 \times [\text{Ic}]$
MAP_{mr8}	15	**0.76**	**67.9**	530	$\text{MAP}_{\text{mr8}} = -619.5 \times 1 + 1725.6 \times [\text{IIIa}] + 161.7 \times [\text{IIIa}'] + 2603.5 \times [\text{IIIb}] - 2069.7 \times [\text{IIIb}'] + 380.3 \times [\text{IIIc}] + 2226.9 \times [\text{IIIc}'] + 730.5 \times [\text{IIa}] + 1028.2 \times [\text{IIa}'] + 2569 \times [\text{IIb}] + 3424.2 \times [\text{IIb}'] + 2734.6 \times [\text{IIc}] + 1830.5 \times [\text{IIc}'] + 1289.3 \times [\text{Ia}] - 854.1 \times [\text{Ib}] - 1745.6 \times [\text{Ic}]$

[a]: The models displayed in blue have the best Siberian-Mongolian data cross-fit.
[b]: The one in red are the most universal models.

2 Supplementary figures

To help the understanding of the limits and uncertainties of our calibrations, the correlation between the climate parameters from the *WorldClim2* modern climate modelling are presented in the figure S1. Then the figure S2 present in three parcels the NMSDB br–GDGTs data set in comparison with the values from the world br–GDGT data bases. Finally, some of the brGDGTs–climate models designed in this study are presented in figure S3 : the mr–models as well as the MBT and CBT models.
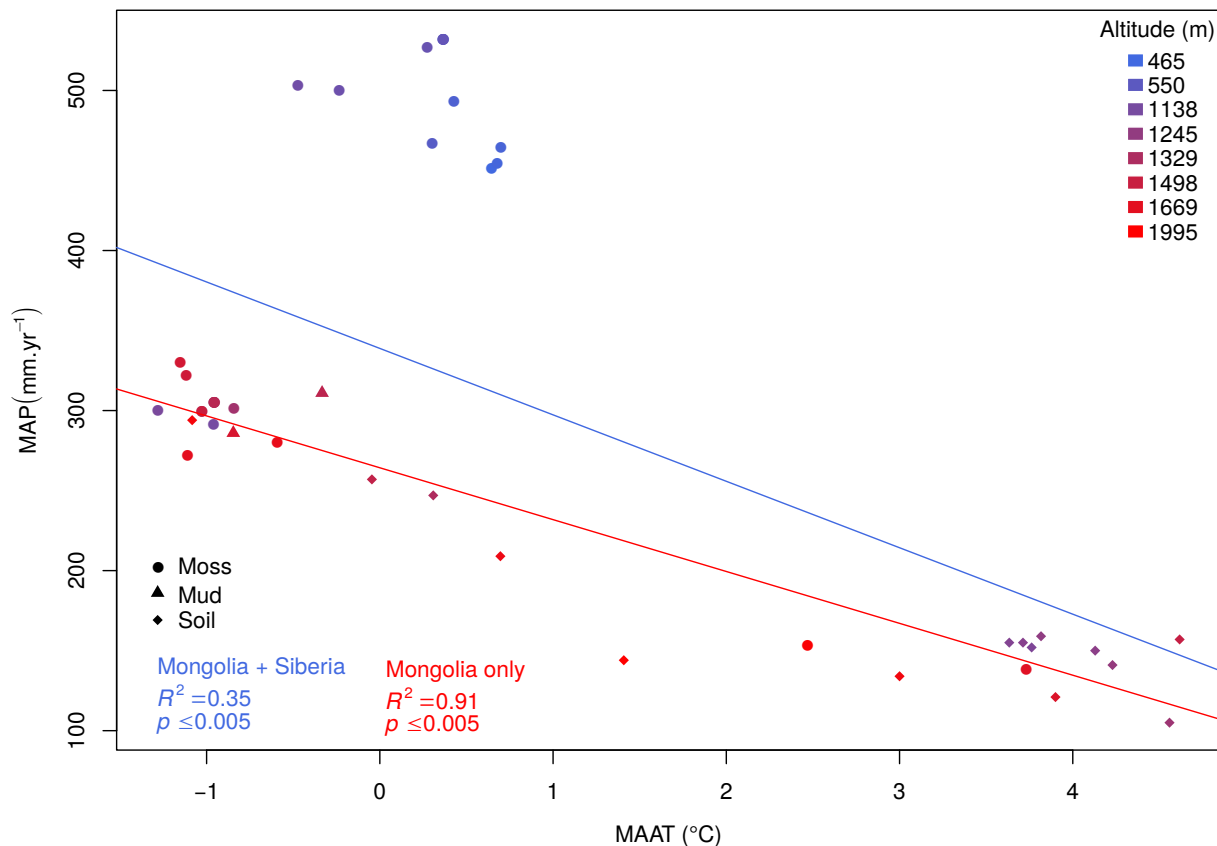

Figure S1. Relation between MAAT and MAP for all the sites of the NMSDB extracted from *WorldClim2* (Fick and Hijmans, 2017). Shapes illustrate the type of sample (dot for moss, triangle for mud and lozenge for soil samples) and the red-blue coloured range highlight the altitude gradient. The two curves display the linear regression of the MAP–MAAT correlation in the full NMSDB (blue) and the Mongolian subplot (red).
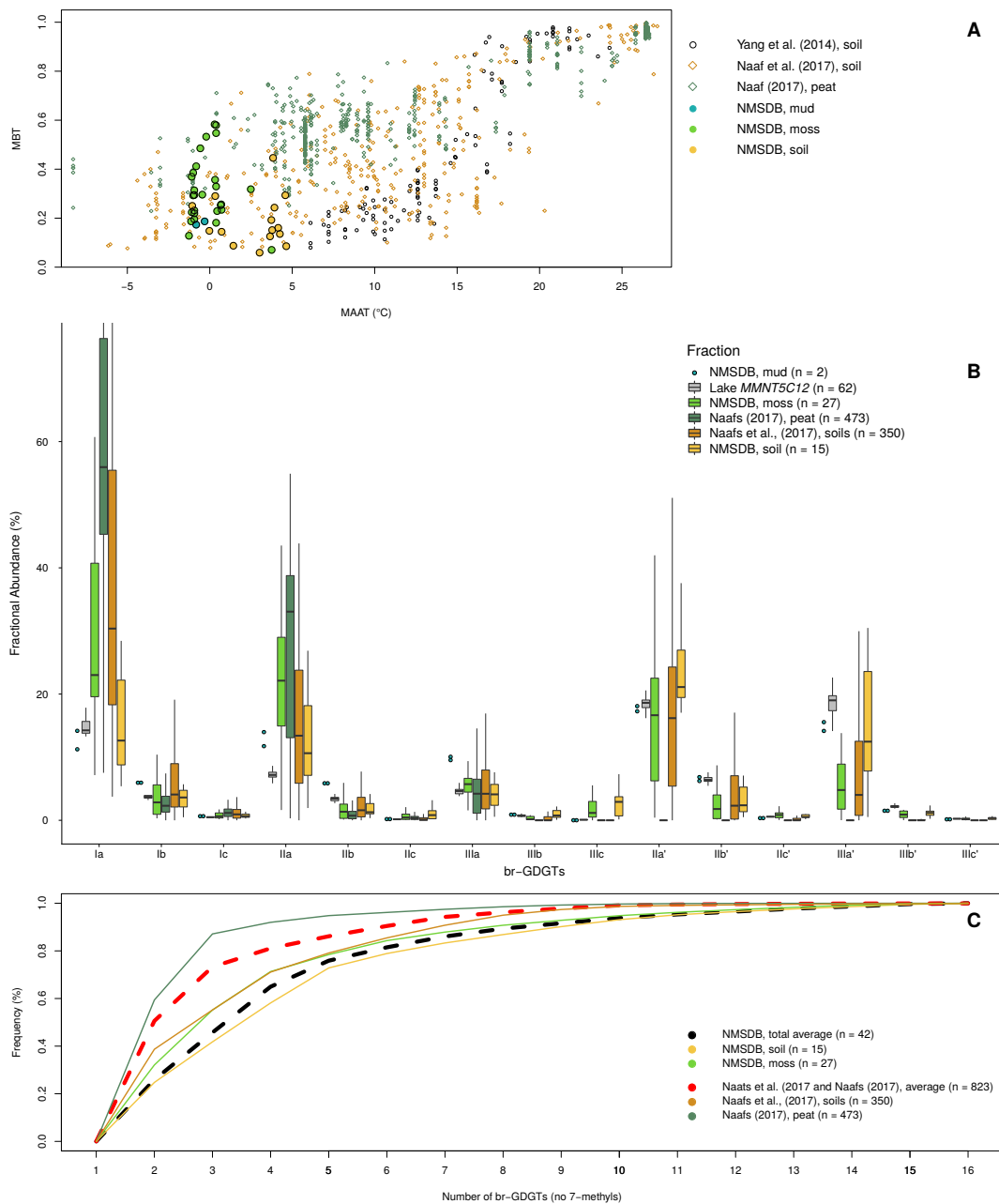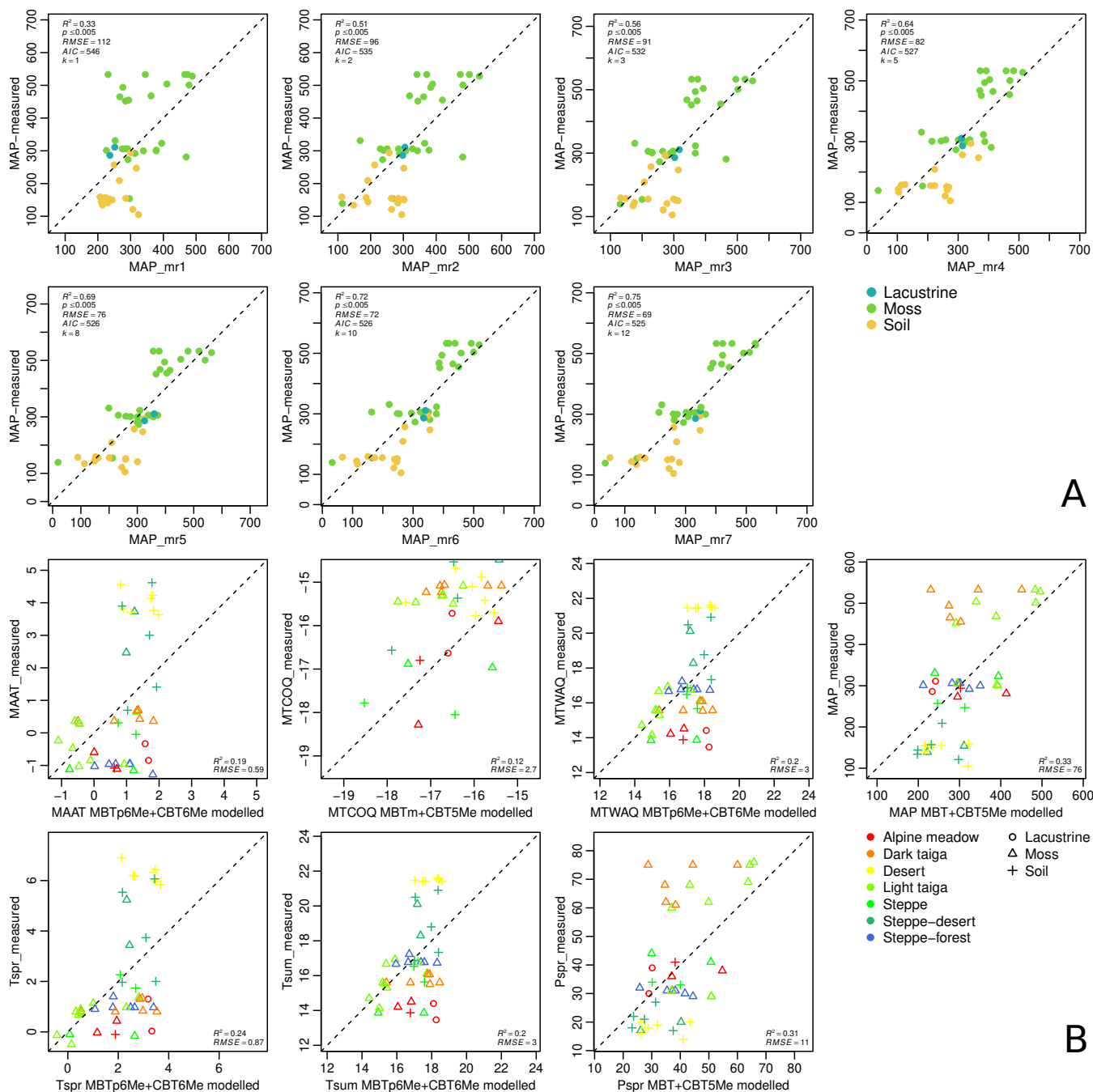
Figure S2. Global comparison between the NMSDB and some world surface brGDGT results. Comparison of the dispersion of the NMSDB samples in front of the global databases for (**A**) the MBT–MAAT relation. **B**: Histogram of the brGDGT fractional abundance. **C**: Cumulative curve of the br–GDGT average values. Global databases from Yang et al. (2014); Naafs et al. (2017); Naafs (2017).

Figure S3. A : Cross-plot for $\mathrm{MAP_{mr}}$ model. The parcels are sorted by increasing parameter number. **B** : Cross-plot for selected climate MBT–CBT models.

References

De Jonge, C., Hopmans, E. C., Zell, C. I., Kim, J.-H., Schouten, S., and Sinninghe Damsté, J. S.: Occurrence and abundance of 6-methyl branched glycerol dialkyl glycerol tetraethers in soils: Implications for palaeoclimate reconstruction, Geochimica et Cosmochimica Acta, 141, 97–112, 2014a.

De Jonge, C., Stadnitskaia, A., Hopmans, E. C., Cherkashov, G., Fedotov, A., and Sinninghe Damsté, J. S.: In situ produced branched dialkyl glycerol tetraethers in suspended particulate matter from the Yenisei River, Eastern Siberia, Geochimica et Cosmochimica Acta, 125, 476–491, 2014b.

Ding, S., Xu, Y., Wang, Y., He, Y., Hou, J., Chen, L., and He, J.-S.: Distribution of branched glycerol dialkyl glycerol tetraethers in surface soils of the Qinghai–Tibetan Plateau: implications of brGDGTs-based proxies in cold and dry regions, Biogeosciences, 12, 3141–3151, 2015.

Fick, S. E. and Hijmans, R. J.: WorldClim 2: new 1-km spatial resolution climate surfaces for global land areas: NEW CLIMATE SURFACES FOR GLOBAL LAND AREAS, International Journal of Climatology, 37, 4302–4315, 2017.

Hopmans, E. C., Weijers, J. W., Schefus s, E., Herfort, L., Damsté, J. S. S., and Schouten, S.: A novel proxy for terrestrial organic matter in sediments based on branched and isoprenoid tetraether lipids, Earth and Planetary Science Letters, 224, 107–116, 2004.

Huguet, A., Fosse, C., Laggoun-Défarge, F., Delarue, F., and Derenne, S.: Effects of a short-term experimental microclimate warming on the abundance and distribution of branched GDGTs in a French peatland, Geochimica et Cosmochimica Acta, 105, 294–315, 2013.

Naafs, B., Gallego-Sala, A., Inglis, G., and Pancost, R.: Refining the global branched glycerol dialkyl glycerol tetraether (brGDGT) soil temperature calibration, Organic Geochemistry, 106, 48–56, 2017.

Naafs, B. D. A.: Global biomarker (GDGT) database for peatlands, https://doi.org/https://doi.org/10.1594/PANGAEA.883765, https://doi.pangaea.de/10.1594/PANGAEA.883765, 2017.

Peterse, F., van der Meer, J., Schouten, S., Weijers, J. W., Fierer, N., Jackson, R. B., Kim, J.-H., and Damsté, J. S. S.: Revised calibration of the MBT–CBT paleotemperature proxy based on branched tetraether membrane lipids in surface soils, Geochimica et Cosmochimica Acta, 96, 215–229, 2012.

Sun, Q., Chu, G., Liu, M., Xie, M., Li, S., Ling, Y., Wang, X., Shi, L., Jia, G., and Lü, H.: Distributions and temperature dependence of branched glycerol dialkyl glycerol tetraethers in recent lacustrine sediments from China and Nepal, Journal of Geophysical Research: Biogeosciences, 116, 2011.

Thomas, E. K., Clemens, S. C., Sun, Y., Huang, Y., Prell, W., Chen, G., Liu, Z., and Loomis, S.: Midlatitude land surface temperature impacts the timing and structure of glacial maxima, Geophysical Research Letters, 44, 984–992, 2017.

Wang, H., Liu, W., and Lu, H.: Appraisal of branched glycerol dialkyl glycerol tetraether-based indices for North China, Organic Geochemistry, 98, 118–130, 2016.

Weijers, J. W., Schouten, S., van den Donker, J. C., Hopmans, E. C., and Damsté, J. S. S.: Environmental controls on bacterial tetraether membrane lipid distribution in soils, Geochimica et Cosmochimica Acta, 71, 703–713, 00503, 2007.

Xiao, W., Wang, Y., Zhou, S., Hu, L., Yang, H., and Xu, Y.: Ubiquitous production of branched glycerol dialkyl glycerol tetraethers (brGDGTs) in global marine environments: a new source indicator for brGDGTs, Biogeosciences, 13, 5883–5894, 2016.

Xie, S., Pancost, R. D., Chen, L., Evershed, R. P., Yang, H., Zhang, K., Huang, J., and Xu, Y.: Microbial lipid records of highly alkaline deposits and enhanced aridity associated with significant uplift of the Tibetan Plateau in the Late Miocene, Geology, 40, 291–294, 00080, 2012.

Yang, H., Pancost, R. D., Dang, X., Zhou, X., Evershed, R. P., Xiao, G., Tang, C., Gao, L., Guo, Z., and Xie, S.: Correlations between microbial tetraether lipids and environmental variables in Chinese soils: Optimizing the paleo-reconstructions in semi-arid and arid regions, Geochimica et Cosmochimica Acta, 126, 49–69, 2014.